# ORBITAL FORMATIONKEEPING WITH DIFFERENTIAL DRAG





C.L. Leonard*
*Adroit Systems, Alexandria, VA*

W.M. Hollister**
*Massachusettes Institute of Technology, Cambridge, MA*

E.V. Bergmann***
*Charles Stark Draper Laboratory, Cambridge, MA*



## Abstract

This paper examines the feasibility of using differential drag between two spacecraft as the means for controlling their relative positions. The equations of relative motion between two satellites are derived and a coordinate transformation is made to reduce the formationkeeping problem to the simultaneous solution of a double integrator and a harmonic oscillator. A simple feedback control law is developed that simultaneously and dependently solves the double integrator and harmonic oscillator; the control law consists of two parts: the main control law and the eccentricity minimizing control scheme. Results are presented of four test cases which show that the control law can drive a satellite from an initial position to a target position and maintain the satellite at that location.

## Nomenclature

$\alpha$ = radial component of harmonic motion due to eccentricity
$\beta$ = circumferential component of harmonic motion due to eccentricity
$\delta, \Phi$ = angles defined in Figure 6 for the eccentricity minimizing control switch algorithm
$\theta_0, \theta_1, \theta_2$ = angles traversed in the $(\alpha, \beta/2)$ plane during the three phases of the eccentricity minimizing control
$a$ = magnitude of differential drag acceleration
$e$ = semi-minor axis of elliptic motion due to eccentricity
$n$ = mean orbital angular velocity of master satellite
$r$ = radius of locus in $(\alpha, \beta/2)$ plane during eccentricity minimizing control
$t$ = time
$x$ = radial position of slave satellite relative to target position
$y$ = circumferential position of slave satellite relative to target position
$\bar{x}$ = average radial position offset of slave satellite relative to target position
$\bar{y}$ = average circumferential position offset of slave satellite relative to target position

## Introduction

Several requirements exist for spacecraft to fly in positions relative to other space vehicles. Space tugs and orbital transfer vehicles may have to place them-

---

* Member of Technical Staff, Member AIAA
** Professor of Aeronautics and Astronautics, Associate Member AIAA
*** Section Chief, Member AIAA

selves at and maintain certain positions with respect to the space station until they are required to perform some task. Space shuttles with replacement crews and new supplies may also have to orbit in specified positions relative to the station before they are allowed to dock. When one satellite must fly in a certain position with respect to another satellite, the two are flying in formation; formationkeeping refers to the active measures taken to keep them in their relative positions. Two aspects of the formation flying problem are considered: the maneuvering of one spacecraft relative to another and the actual formationkeeping.

Controllers for formationkeeping were developed by R. Vassar and R. Sherwood [1] and D. Redding, N. Adams and E. Kubiak [2]. Both studies assumed that the actuators for formationkeeping were chemical thrusters; the jets provided sufficiently high thrust to allow the control $\Delta v$'s to be treated as impulsive changes in velocity. Thrust was available along all three translational axes. The control laws were developed using optimal control theory; the first study optimized thruster firing frequency and the second minimized fuel consumption.

By convention, the satellite that takes active control measures to remain in a specific location relative to another spacecraft is called the slave satellite; the spacecraft on which the slave is flying formation is called the master satellite. When differential drag is used to formationkeep, both vehicles may take active measures to retain their relative positions; in this case, one satellite is arbitrarily deemed the master and the other is the slave.

Differential drag between a pair of satellites is the difference in drag per unit mass acting upon each of the satellites. If the satellites are passing through similar density atmospheres with similar velocities, then any differential drag is due to different ballistic coefficients of the vehicles.

In this paper it is assumed that atmospheric density is uniform and that the velocities and ballistic coefficients of the satellites are initially equal. Differential drag is created through the use of drag plates attached to both of the satellites. The angle of attack of each drag plate can be chosen to be 0 or 90 degrees, resulting in on-off control. When the drag plate of both spacecraft are at a 0 or 90 degree angle of attack, no differential drag is created; this is referred to as zero differential drag. Setting the angle of attack of the drag plate connected to the master satellite at 90 degrees and the angle of attack of the plate connected to the slave at 0 degrees, creates positive differential drag and acts as a force along the velocity vector. Setting the angle of attack of the plate connected to the master at 0 degrees and the angle of attack of the plate connected to the slave at 90 degrees, creates negative differential drag and acts as a force opposite to the velocity vector. The magnitude of the differential drag acceleration created was estimated to be $54 \times 10^{-6}$ ft/sec$^2$; this value was calculated by using drag information obtained from skylab data [3], a 13' x 270' drag plate as sized in Reference [4] and a formationkeeping altitude of 270 nautical miles.

Reasons to use differential drag as an actuator in formationkeeping include:

* plumes from jet firings may impinge upon the master satellite, imparting some undesired motion or contaminating solar panels.
* an impulsive jet firing may disturb a manufacturing process on the slave satellite; the accelerations created by differential drag are much smaller than those that arise from jet firings.

* possible fuel savings.

Additional assumptions made in the formulation of the problem are that a change of angle of attack of the drag plate does not affect the attitude of the satellite, that the angle of the drag plate an be changed instantaneously, and that no lift is generated.

## Equations of Motion

The desired position of the slave satellite with respect to the master will be the origin of the target reference coordinate system, shown in Figure 1. It is assumed that the origin is a reference circular orbit. The $x$ direction will be measured along the radius vector to the target from the center of the earth, with the direction away from the earth being positive.

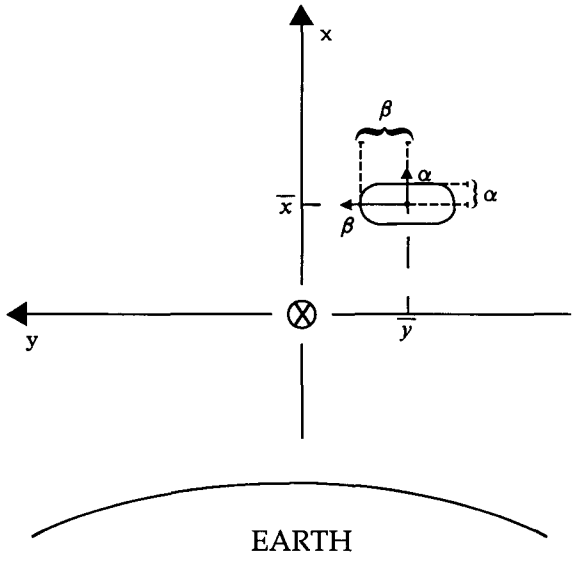


*Figure 1: Target Reference Coordinate System.*

The $y$ direction will be measured along the velocity vector of the target. The third axis, $z$, is normal to the orbit plane, forming a right handed coordinate system.

Since the relative separation of the two satellites is small compared to the orbital radius, the linearized equations of Hill [5] are valid for a circular orbit.

$$\ddot{x} = 2n\dot{y} + 3n^2x + F_x/m \qquad (1)$$

$$\ddot{y} = -2n\dot{x} + F_y/m \qquad (2)$$

where $n$ is the mean orbital angular motion of the master satellite, $F_x$ and $F_y$ are the forces applied to the satellite in the $x$ and $y$ directions respectively and $m$ is the satellite mass. $F_x$ is equal to zero as no lift is generated and $F_y$ is equal to the differential drag; it is assumed that the values which the differential drag can have are $a$, 0, or $-a$. When the master satellite has the greater drag, $a$ is positive. With equal drag, $a$ is zero. When the slave satellite has the greater drag, $a$ is negative.

Unforced solutions to these equations have been presented by several authors [6] [7] [8] and are given in state variable form in Table 1.

The unforced orbit is a two by one ellipse whose center maintains constant altitude difference, $\bar{x}$, with the target position; the center of the ellipse moves ahead or behind of the target position with a relative velocity, $\dot{\bar{y}}$, that is a function of the average altitude difference. A coordinate transformation can be defined as follows:

$$\begin{bmatrix} x \\ y \\ \dot{x} \\ \dot{y} \end{bmatrix} = \begin{bmatrix} 4-3\cos nt & 0 & \frac{1}{n}\sin nt & -\frac{2}{n}\cos nt+\frac{2}{n} \\ 6\sin nt-6nt & 1 & \frac{2}{n}\cos nt-\frac{2}{n} & \frac{4}{n}\sin nt-3t \\ 3n\sin nt & 0 & \cos nt & 2\sin nt \\ 6n\cos nt-6n & 0 & -2\sin nt & 4\cos nt-3 \end{bmatrix} \begin{bmatrix} x_0 \\ y_0 \\ \dot{x}_0 \\ \dot{y}_0 \end{bmatrix}$$

*Table 1: Unforced solution of Hill's Equations in state variable form.*

$$\bar{x} = 4x + 2\dot{y}/n \quad (3)$$

$$\bar{y} = y - 2\dot{x}/n \quad (4)$$

$$\alpha = -3x - 2\dot{y}/n = x - \bar{x} \quad (5)$$

$$\beta = 2\dot{x}/n = y - \bar{y} \quad (6)$$

The eccentricity of the orbit is proportional to the linear dimensions of the two by one ellipse which will be measured by

$$e \equiv [\ \alpha^2 + (\beta/2)^2\ ]^{1/2} \quad (7)$$

The transformation leads to two uncoupled, second-order, linear differential equations

$$\ddot{\bar{y}} = -3a \quad (8)$$

$$\ddot{\beta} + n^2\beta = 4a \quad (9)$$

Controlling $\bar{y}$ and $\beta$ effectively controls $\bar{x}$ and $\alpha$ as

$$\bar{x} = -2\dot{\bar{y}}/(3n) \quad (10)$$

and

$$\alpha = -\dot{\beta}/(2n) \quad (11)$$

Equation 8 is a double integrator and Equation 9 is a harmonic oscillator. The forced solutions are obtained as

$$\bar{x}(t) = \bar{x}_0 + 2at/n \quad (12)$$

$$\bar{y}(t) = \bar{y}_0 - 3n\bar{x}_0 t/2 - 3at^2/2 \quad (13)$$

$$\alpha(t) = \alpha_0 \cos nt + (\tfrac{\beta}{2}_0 - \tfrac{2a}{n^2})\sin nt \quad (14)$$

$$\tfrac{\beta}{2}(t) = (\tfrac{\beta}{2}_0 - \tfrac{2a}{n^2})\cos nt - \alpha_0 \sin nt + \tfrac{2a}{n^2} \quad (15)$$

Time optimal control for each system alone is well known [9] [10], using switch curves in the phase plane. However, here the two control laws must be combined in such a way that all four states are driven to the origin simultaneously.

## The Effect of Control in the Phase Plane

In the $(\bar{x},\bar{y})$ plane the forced solutions plot as parabolas. Positive differential drag will cause the state to move along the trajectories represented by the solid lines in Figure 2; negative differential drag will cause the state to move along the dashed trajectories. Zero differential drag would cause the state to move parallel to the $\bar{y}$ axis at a rate that is a function of $\bar{x}$; the movement would be in the negative $\bar{y}$ direction if $\bar{x}$ were positive and in the positive $\bar{y}$ direction if $\bar{x}$ were negative.

In the $(\alpha,\beta)$ plane the loci are two by one ellipses, centered on the points $(4a/n^2,0)$ and $(-4a/n^2,0)$ caused by positive and negative drag respectively. By plotting $\beta/2$ instead of $\beta$, the loci become circles centered on the points $(2a/n^2,0)$ and $(-2a/n^2,0)$ with a radius arm of magnitude $e$ that rotates at the angular rate $n$. Positive differential drag will cause the state to move along the trajectories represented by the solid lines in Figure 3; negative differential drag will cause the state to move along the dashed trajectories. Zero differential drag would cause the state to circle about the origin.

When control is switched, the instantaneous values of the four

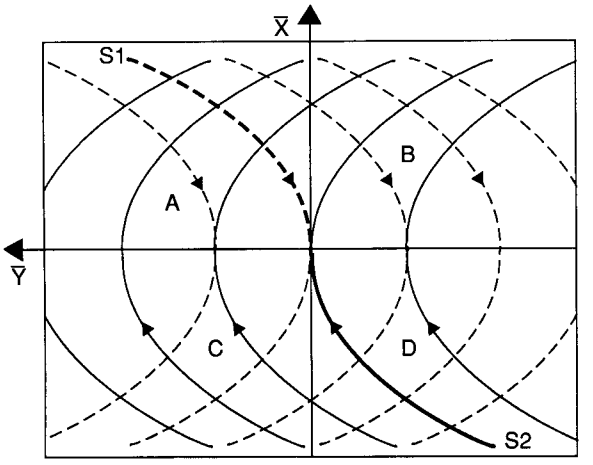


Figure 2: Control Trajectories, Switch Curves and Control Areas in the $(\bar{x},\bar{y})$ plane.

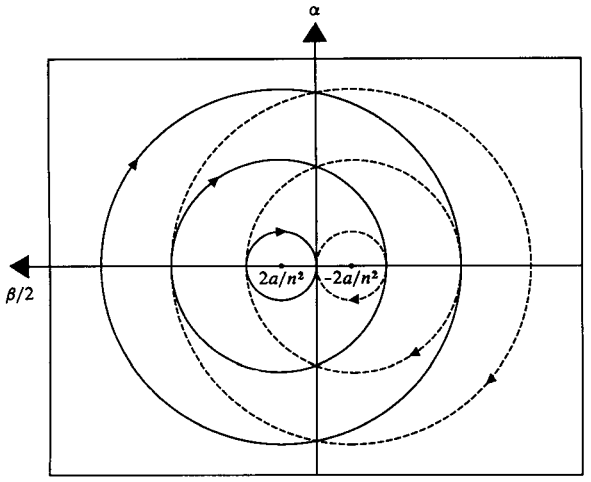


*Figure 3: Control Trajectories in the* $(\alpha,\beta/2)$ *plane.*

state variables remain constant, but future values are determined by the appropriate new trajectory.

The primary interest in this application centered on feasibility rather than optimality. The objective was to demonstrate that a relatively simple control system without extensive iterations would actually work. This was carried out in Reference [11] and will be presented in an abbreviated form in the remainder of this paper.

## Formation Maneuvering

A two part control law was developed to drive the true average relative position to zero and reduce the eccentricity as much as possible. If the eccentricity is driven to zero while the average relative position is non-zero, the average relative position can diverge. Consequently, the control strategy used is to first bring the average position of the slave to that of the target while decreasing eccentricity as much as feasible; this process is called the main control law. After the average position has been brought to zero, the eccentricity is further reduced using the eccentricity minimizing control scheme.

### The Main Control Law

Once the average position is moving toward the origin, the control law used differs from the double integrator minimum-time solution [9] in order to reduce eccentricity.

If the average position lies in areas B or C as shown in Figure 2, then the sign of the control is chosen to move the state along a parabola toward the appropriate switch curve. This constant control in the B or C region will cause the state to circle about the appropriate point in the $(\alpha,\beta/2)$ plane. For example, if the average position were in area B, a negative differential drag would be commanded to move the average position toward the D region in the $(\bar{x},\bar{y})$ plane; the resultant trajectory in the $(\alpha,\beta/2)$ plane would be a circle around $(-2a/n^2,0)$.

The control will be switched when $\bar{y}>0$ and $\bar{x}<S1$ or when $\bar{y}<0$ and $\bar{x}>S2$. Since

$$\frac{d(e^2)}{dt} = \frac{-4a\alpha}{n} \qquad (16)$$

the eccentricity is decreased whenever the control, $a$, has the same sign as $\alpha$. For $a$ to have the same sign as $\alpha$, $a$ must change sign when $\alpha$ changes sign, which is twice each orbit. As a result, the state will move in a sawtooth pattern toward the appropriate switch curve in the $(\bar{x},\bar{y})$ plane. For the sawtooth action to move the slave toward the target, the average position during the sawtooth must stay in area A or D.

An exception to $a$ changing sign twice each orbit occurs when the eccentricity is small. When $e<4a/n^2$ the sawtooth maneuver can at best bound the eccentricity; this is done by $a$ switching control once per orbit and is explained in detail in Reference [11].

Once the switch curve in the

$(\overline{x},\overline{y})$ plane is reached, the control that brings the state to the origin is exercised immediately, no matter what the consequence to the eccentricity. After the origin is reached, the eccentricity minimizing control scheme is used to reduce any remaining eccentricity.

The Eccentricity Minimizing Control Scheme

The eccentricity minimizing control scheme was designed to reduce the eccentricity as much as possible without altering the final average position of the slave. It approximates the harmonic oscillator minimum-time solution [10].

In eccentricity minimizing control the commanded differential drag is initially zero, which keeps the average position of the slave at the target and results in the state circling about the origin in the $(\alpha,\beta/2)$ plane.

A hat shaped maneuver is then performed in the $(\overline{x},\overline{y})$ plane. The first two legs of the hat are the trajectories caused by opposite commanded controls; a slight difference in the duration of the controls causes an offset from the $\overline{y}$ axis at the end of the second leg as can be seen in Figure 4. The base of the hat is formed by the unforced motion or drift of the state caused by the position offset $\overline{x}$; during this phase of the eccentricity mini-mizing control scheme the differential drag is zero.

The angle traversed by the state in the $(\alpha,\beta/2)$ plane while the differential drag is initially zero is $\theta_0$. The angle traversed by the state during the first interval of non-zero commanded drag will be referred to as $\theta_1$; the angle corresponding to the subsequent opposite drag will be known as $\theta_2$ as shown in Figure 5. For the eccentricity minimizing control scheme to work, the second leg of the hat in the $(\overline{x},\overline{y})$ plane must be longer than the first leg so that the state crosses the $\overline{y}$ axis and the zero thrust orbital motion brings the average position back toward the origin. For the second leg to be longer than the first leg, the angle that the second leg traverses in the $(\alpha,\beta/2)$ plane must be larger than the angle of the first leg; $\theta_2$ must be larger than $\theta_1$.

The difference between $\theta_1$ and $\theta_2$ affects the closing rate of the slave during the drift phase of the hat maneuver and the minimum eccentricity that the control law can achieve. For $e>4a/n^2$, $\theta_2 - \theta_1$ was set to be 20 degrees to insure a large closing rate of the average position of the slave toward the target in the unthrusted phase of the maneuver. For $e<4a/n^2$, the

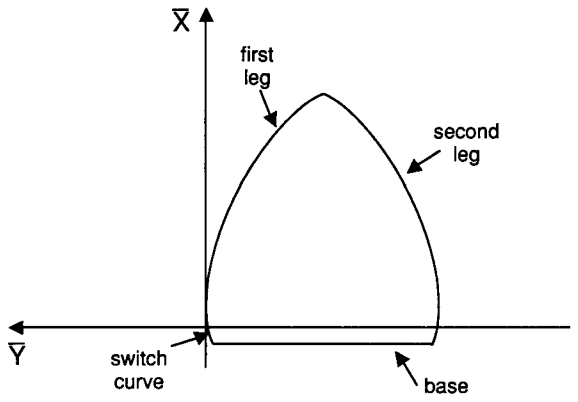


*Figure 4: The Hat Maneuver of the Eccentricity Minimizing Control Scheme in the $(\overline{x},\overline{y})$ plane.*

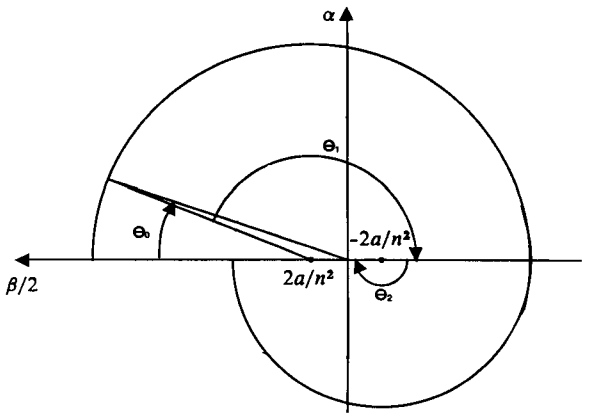


*Figure 5: The Switch Decision Process for Large Eccentricity in the $(\alpha,\beta/2)$ plane.*

difference was chosen as 10 degrees to allow an acceptable final eccentricity.

For $e>4a/n^2$, $\theta_2$ is given as 180 degrees by the phase plane for the harmonic oscillator; thus $\theta_1$ equals 160 degrees and $\theta_0$ is 20 degrees. The commanded drag will switch from zero to either plus or minus $a$ when $\theta_0$ equals 20 degrees. For $\alpha$ greater than zero the proper control will be positive. This first switch will reduce the eccentricity and form the first leg of the hat. The next switch will occur at the $\beta/2$ axis after the angle $\theta_1$ has been passed; it will command a change in sign. This action will reduce the eccentricity once again and form the second leg of the hat. When the $\beta/2$ axis is reached again (corresponding to a transferred $\theta_2$ of 180 degrees), the drag is commanded to be zero. The states in the $(\alpha,\beta/2)$ plane will then circle about the origin and the states in the $(\bar{x},\bar{y})$ plane will drift toward the origin, forming the base of the hat.

When the drifting slave encounters the switch curve in the $(\bar{x},\bar{y})$ plane, the appropriate drag control will drive the average position of the slave to the target. The strategy will be repeated until the eccentricity has been reduced enough to go through the eccentricity minimizing control scheme for $e<4a/n^2$.

For $e<4a/n^2$ the eccentricity of the system determines the values of $\theta_1$, $\theta_2$ and the $\theta_0$ at which the first switch to non-zero drag will occur. The algorithm to select the proper values of $\theta_1$, $\theta_2$ and $\theta_0$ follows from the geometry in Figure 6.

$$\theta_0 = \tan^{-1}(2\alpha/\beta) \tag{17}$$

$$r = [e^2+(2a/n^2)^2-2e(2a/n^2)\cos\theta_0]^{1/2} \tag{18}$$

$$\delta = \sin^{-1}\left[\frac{e}{r}\sin\theta_0\right] \tag{19}$$

$$\Phi = \cos^{-1}\left[\frac{r^2+(4a/n^2)^2-(2a/n^2)^2}{2r(4a/n^2)}\right] \tag{20}$$

$$\theta_1 = \delta + \Phi \tag{21}$$

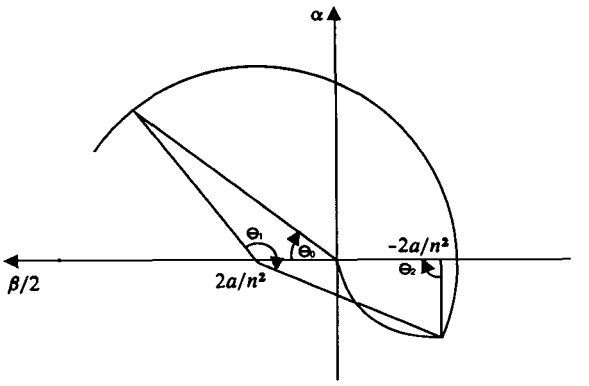


*Figure 6: Geometry in the $(\alpha,\beta/2)$ plane for the Switch Algorithm in the Decision Making Process for Small Eccentricities.*

$$\theta_2 = \sin^{-1}\left[\frac{r\sin\Phi}{2a/n^2}\right] \tag{22}$$

The first switch to non-zero differential drag is made when $\theta_2$ is 10 degrees greater than $\theta_1$. The second switch occurs when the current value of $e$ satisfies

$$e^2 = 2(2a/n^2)^2 - 2(2a/n^2)^2\cos\theta_2 \tag{23}$$

When the eccentricity reaches zero, the drift phase begins. A switch is made to zero commanded drag; the eccentricity stays at zero and the unthrusted motion of the slave corresponds to the base of the hat in the $(\bar{x},\bar{y})$ plane.

When the state crosses the switch curve in the $(\bar{x},\bar{y})$ plane, the appropriate drag control will drive the average position of the slave to the target. After the average position reaches that of the target, the final eccentricity should be acceptable as determined by the choice of the 10 degrees difference between $\theta_2$ and $\theta_1$.

## Simulations

The first simulation was based on the equations of motion developed in this paper. The differential drag was given a constant value of .1944 ft/min² based on References [3] and [4].

The second simulation used the Space Systems Simulator at the Charles Stark Draper Laboratory, an engineering tool used in support of shuttle, space station and Department of Defense payloads. The motion of both the target and the slave were integrated in spherical then converted into inertial coordinates; the position and velocity of the target and slave were differenced to calculate $\overline{y}$, $\overline{x}$, $\alpha$ and $\beta$. The magnitude of the differential drag created by a 90 degree deflection of the drag plate was computed once using a Jacchia atmosphere, then assumed constant thereafter.

Eight sets of initial conditions were tested in both simulations. The control scheme worked satisfactorily in all cases. Because of space only three cases using the above equations are shown in Figures 7-11. Figures 7, 8, and 9 show the

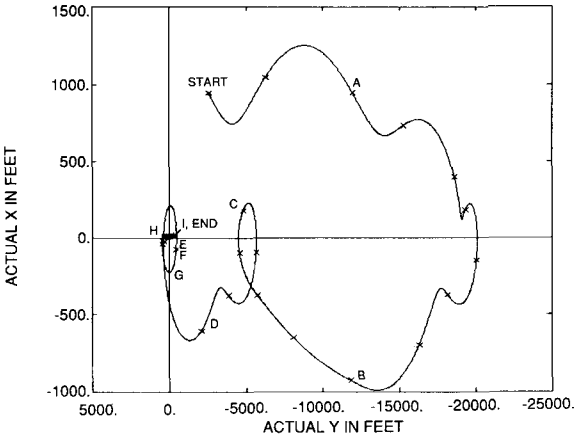


| position | simulation time (min) | commanded control | duration of control (min) |
|---|---|---|---|
| START | 0.0 | a=0 | 92.0 |
| A | 92.0 | a>0 | 331.2 |
| B | 423.2 | a<0 | 190.8 |
| C | 614.0 | a>0 | 124.8 |
| D | 738.8 | a<0 | 93.6 |
| • E | 832.4 | a=0 | 33.6 |
| F | 866.0 | a>0 | 26.4 |
| G | 892.4 | a<0 | 28.8 |
| H | 921.2 | a=0 | 484.8 |
| I | 1406.0 | a>0 | 0.8 |

• start of eccentricity minimizing control scheme

*Figure 7: Motion in the $(x,y)$ Plane for Case 1.*

$(x,y)$ plane, $(\alpha,\beta/2)$ plane and the motion in the $(\overline{x},\overline{y})$ plane respectively for a given case to illustrate the separate control laws and their final effect on the actual motion of the spacecraft. Figures 10 and 11 show the motion in the $(x,y)$ plane for two more cases. The other test cases are similar; details of all the results are available in Reference [11].

## Position Maintenance

Two methods were used to keep the slave at the target position using differential drag. One simply restarted the control scheme once the slave had drifted 10 feet away from the origin. The other used two rules, collectively referred to as the limit cycle control law: (1) if

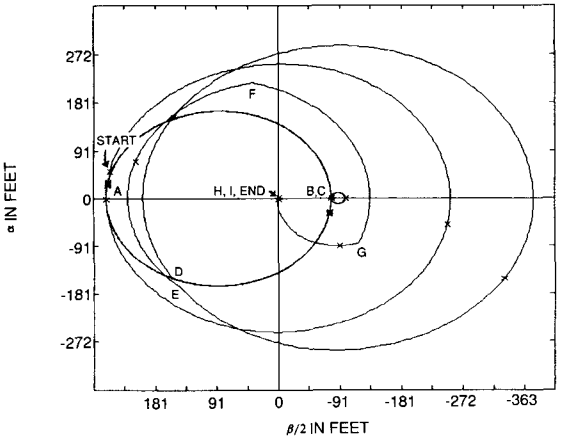


*Figure 8: Motion in the $(\alpha,\beta/2)$ Plane for Case 1.*

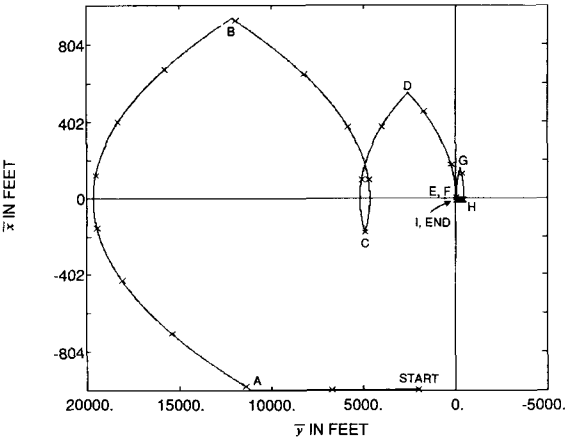


*Figure 9: Motion in the $(\overline{x},\overline{y})$ Plane for Case 1.*

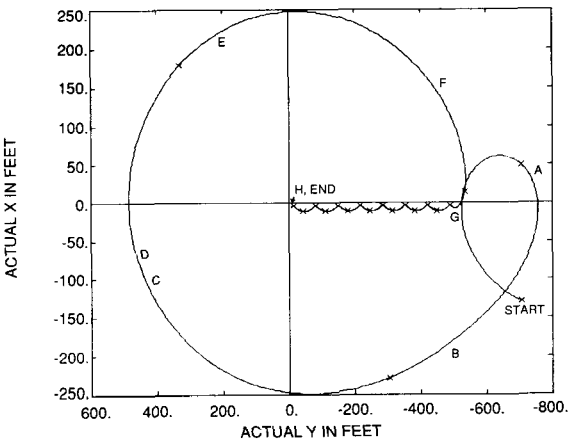


| position | simulation time (min) | commanded control | duration of control (min) |
|---|---|---|---|
| START | 0.0 | a=0 | 64.0 |
| A | 64.0 | a>0 | 24.4 |
| B | 88.4 | a<0 | 35.6 |
| C | 124.0 | a>0 | 3.6 |
| * D | 127.6 | a=0 | 21.2 |
| E | 148.8 | a<0 | 28.4 |
| F | 177.2 | a>0 | 30.4 |
| G | 207.6 | a=0 | 704.0 |
| H | 911.6 | a<0 | 0.4 |

* start of eccentricity minimizing control scheme

*Figure 10: Motion in the (x,y) Plane for Case 2.*

$\overline{x}$ is negative when $\overline{y}$ becomes more than 1 foot away from the origin, a positive drag is commanded for one 0.4 minute time step, (2) if $\overline{x}$ is positive when $\overline{y}$ becomes more than 1 foot away from the origin, a negative drag is commanded for one 0.4 minute time step. The acceptable positions for $\overline{x}$ after being placed at the origin by the formation maneuvering control laws are such that the proper drag, commanded to last for 0.4 minutes, will send $\overline{x}$ to the other side of the $\overline{y}$ axis; this maneuver will reverse the direction that the slave is drifting with respect to the target.

## Simulations

The simulation of the position maintenance was based on Equations 12, 13, 14 and 15. Three sets of initial conditions were tested for

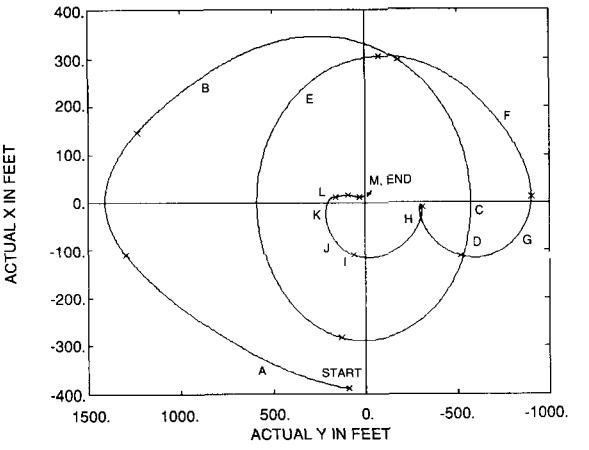


| position | simulation time (min) | commanded control | duration of control (min) |
|---|---|---|---|
| START | 0.0 | a=0 | 16.8 |
| A | 16.8 | a<0 | 98.0 |
| B | 114.8 | a>0 | 52.4 |
| C | 167.2 | a<0 | 4.8 |
| * D | 172.0 | a=0 | 44.4 |
| E | 216.4 | a<0 | 37.6 |
| F | 254.0 | a>0 | 47.2 |
| G | 301.2 | a=0 | 115.6 |
| H | 416.8 | a<0 | 9.6 |
| I | 426.4 | a=0 | 2.4 |
| J | 428.8 | a>0 | 16.4 |
| K | 445.2 | a<0 | 19.6 |
| L | 464.8 | a=0 | 124.4 |
| M | 589.2 | a>0 | 1.6 |

* start of eccentricity minimizing control scheme

*Figure 11: Motion in the (x,y) Plane for Case 3.*

both control methods. Because of space, only one case per method is shown in Figures 12 and 13. Figure 12 shows the results for when the formation man- euvering control law is restarted; Figure 13 presents the results for the limit cycle control law. The other test cases are similar; details of all the results are available in Reference [11].

## Conclusions

The formationkeeping problem has been formulated as the simultaneous solution of a double integrator and a harmonic oscillator. The double integrator models the average position of the slave relative to the target; the harmonic oscillator models the eccentricity of the

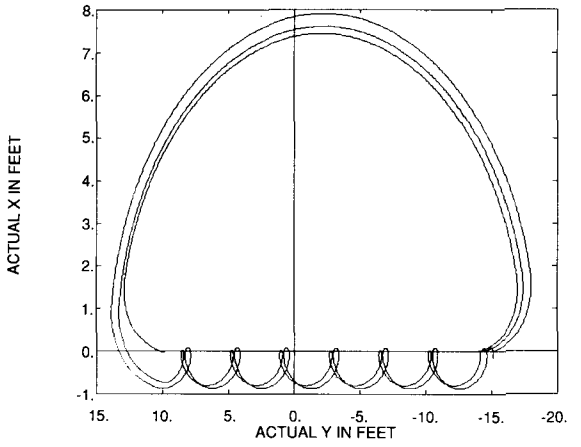


Figure 12: Position Maintenance by Restarting the Control Scheme.

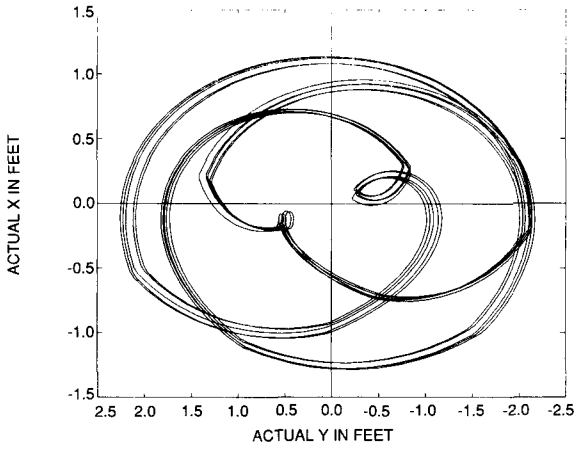


*Figure 13: Position Maintenance using the Limit Cycle Control Law.*

slave. Solving the double integrator and harmonic oscillator concurrently leads to the positioning of the slave at the target.

The main control law drives the average position of the slave to that of the target while minimizing eccentricity as much as possible. The eccentricity minimizing control scheme is activated once the average position of the slave is at the target; its purpose is to reduce the eccentricity of the slave as much as possible without jeopardizing its final average position.

The control law was tested using eight sets of initial conditions and two different simulations. The control law was capable of moving a slave satellite from an arbitrary initial position to a specified orbiting target. All cases tested were driven to the target in less than 24 hours despite the fact that the control did not represent the minimum time solution.

Two methods were tested for position maintenance. One activated the main control law when the slave drifted a certain distance from the origin; the other used the limit cycle control law. The first was able to keep the slave within 18 feet of the origin, while the limit cycle control law kept the slave within 4.17 feet of the origin.

The time optimal solution could be found for the formation flying problem for a limited range of $e$. Assuming k segments of time that have alternating sign of the control, successive applications of Equations 12, 13, 14 and 15 give the final state as a function of the initial state and the k time segments; using the origin as the final state and knowing the initial position, this iterative process can be used to find the optimum duration of the k time segments.

A linear controller (with saturation) could be designed for position maintenance if the angle of attack of the drag plates was assumed to vary continuously from -90 to 90 degrees.

## References

[1] Vassar, R.H. and Sherwood, R.B. "Formationkeeping for a Pair of Satellites in a Circular Orbit" AIAA Journal of Guidance and Control, March-April 1985: 235-242.

[2] Redding, David C., Adams, Neil J., and Kubiak, Edward T. "Linear Quadratic Stationkeeping for the STS Orbiter", Charles Stark Draper Laboratory Report CSDL-R-1879, June 1986.

[3] Skylab Program Operational Data Books Vols II and IV, NASA MSC-01549, 1971.

[4] Vargas, Tina F. "Attitude Control Augmentation of Spacecraft in Low Earth Orbit Utilising Aerodynamic Forces" Master of Science Thesis, M.I.T., December 1982

[5] Hill, George W. "Researches in the Lunar Theory". American Journal of Mathematics. Vol.1, No1. 1878: 5-26

[6] Hollister, Walter M. "The Design of a Control System for the Terminal Phase of a Satellite Rendezvous" Master of Science Thesis, M.I.T., June 1959

[7] Wheelon, Albert D. "Midcourse and Terminal Guidance." in Space Technology. Ed. Seifert, Howard. New York: John Wiley & Sons, 1959.

[8] Clohessy, W.H. and Wiltshire R.S. "Terminal Guidance Systems for Satellite Rendezvous." Journal of the Aerospace Science Sept. 1960: 653-658,674.

[9] Bryson, A.E. and Ho, Y.C. Applied Optimal Control. Waltham, MA: Blaisdell Publishing Company, 1969

[10] Athans, M. and Falb, P.L. Optimal Control. New York: McGraw-Hill, 1966

[11] Leonard, Carolina L., "Formationkeeping of Spacecraft Via Differential Drag" Master of Science Thesis, M.I.T., July 1986